# Temporal evolution of surface and sub-surface geochemistry and microbial communities of Pb-rich mine tailings during phytostabilization: A one-year pilot-scale study

Hugues Thouin, Marie-Paule Norini, Fabienne Battaglia-Brunet, Pascale Gautret, Marc Crampon, Lydie Le Forestier

# Temporal evolution of surface and sub-surface geochemistry and microbial communities of Pb-rich mine tailings during phytostabilization: a one-year pilot-scale study

Authors:

Hugues Thouin[b‡], Marie-Paule Norini[a,b], Fabienne Battaglia-Brunet[a,b], Pascale Gautret[a], Marc Crampon[b], Lydie Le Forestier[a]

‡Corresponding author

[a]Université d'Orléans, CNRS, BRGM, ISTO, UMR 7327, 45071 Orléans, France.

[b]BRGM, BP 36009, 45060 Orléans Cedex 2, France.

## Graphical abstract

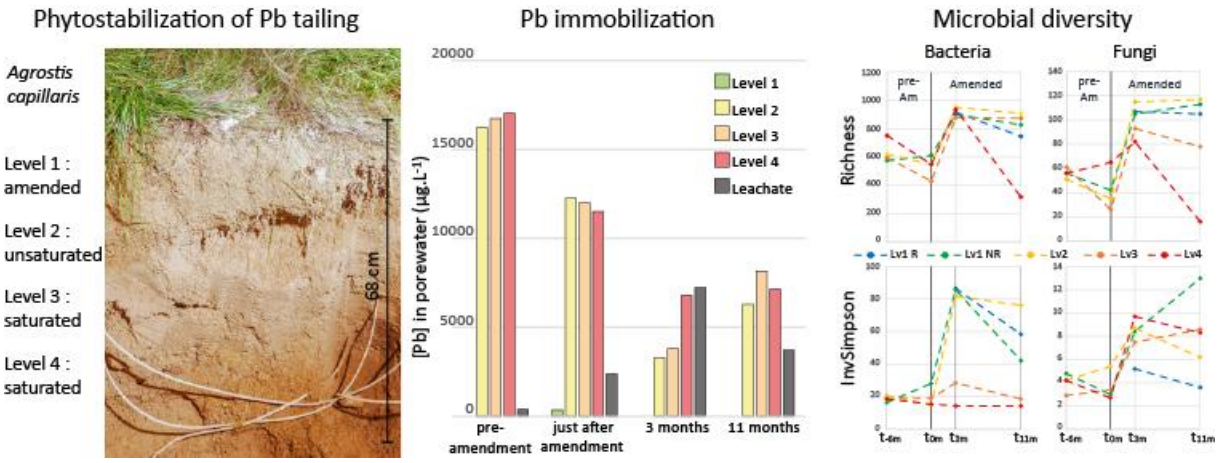

## Abstract

Old mine waste repositories can present health and/or environmental issues linked to their erosion, inducing dissemination of metals and metalloids in air and water that can be attenuated through phytostabilization. Here, the effect of this widespread phytomanagement option on the biogeochemistry of a Pb-rich mine waste was evaluated with a laboratory pilot-scale experiment giving access to the non-saturated and saturated zones below the rhizosphere compartment. Amendment of the tailings surface with biochar, manure and iron-oxide-rich ochre promoted growth of the seeded *Agrostis capillaris* plants. These events were accompanied by an increase of pH and a decrease of Pb concentration in pore water of the surface layer, and by a transient increase of Pb, Zn, and Ba concentrations in the deeper saturated levels. Macroscopic and microscopic observations (SEM) suggest that Pb was immobilized in *A. capillaris* rhizosphere through mechanical entrapment of tailing particles. Microbial taxonomic and metabolic diversities increased in the amended phytostabilized surface levels, with an increase of the proportion of heterotrophic micro-organisms. Below the surface, a transient modification of microbial communities was observed in the non-saturated and saturated levels, however 11 months after seeding, the prokaryotic community of the deepest saturated zone was close to that of the initial tailings. pH and water saturation seemed to be the main parameters driving prokaryotic communities' structures. Results obtained at pilot-scale will help to precisely evaluate the impacts of phytostabilization on the temporal evolution of reactions driving the fate of pollutants inside the tailings dumps.



**Key words:** mine tailings, metals, assisted phytostabilization, laboratory pilot, microbial diversity.

# 1 Introduction

Unrestored mine tailing sites are a worldwide problem since they generally remain bare for decades or even centuries. For abandoned mine tailing heaps, the establishment of a spontaneous vegetation cover is usually considered beneficial as it represents a sort of phytostabilization (Houben et al., 2013). Indeed, revegetation of these degraded sites appears as a suitable long-term solution: the plant cover limits eolian dispersion, while the roots prevent water erosion and leaching, and provide a rhizosphere wherein metals can precipitate and stabilize (Mendez and Maier, 2008). However, for lead (Pb)/zinc (Zn) mine sites, metal toxicity, especially available Pb, nutrient deficiency, and poor physical structure of the substrate are major constraints for plant establishment and colonization (Ye et al., 2002). Therefore, a suitable strategy consists of aided phytostabilization by using pioneer plants (Lago-Vila et al., 2019) coupled with efficient organic and inorganic amendments (Sikdar et al., 2020).

In this context, numerous laboratory studies with pot experiments have recently been devoted to test the efficiency of plants and several amendments, alone or in combination, on Pb and Zn retention and plant growth in mine tailings (Ciarkowska et al., 2017; Al-Lami et al., 2019; Norini et al., 2019; Gao et al., 2020). Although different combinations may rapidly be tested, these pot experiments only focused on plant biomass and metal availability in the rhizosphere area, and are far from the field scale.

Other small-scale experiments include laboratory percolation tests enabling to measure/assess the transfer of contaminants through mine residues and to evaluate the effect of amendments (Rodriguez et al., 2018; Thouin et al., 2019), whereas influence of water saturation can be studied in columns (Ouangrawa et al., 2010). These systems are well constrained and they give insight on small-scale processes but it is necessary to increase the scale in order to understand interactions between different compartments and reflect field conditions.

In this regard, field experiments have been conducted to optimize the combination of plants and amendments in phytostabilization of metal(loid)s pollutants in mine sites (Yang et al., 2016; Acosta et al., 2018; Li et al., 2019). However, some key parameters could not be precisely controlled and accounted for, such as soil water saturation and incoming water flow. Moreover, some types of samples, such as pore water at different depths are difficult to collect during on-site studies and spatial heterogeneities of mine tailings often represent an obstacle for the interpretation of results obtained on-site (Constantinescu et al., 2019).

To overcome these limitations, lysimeters directly installed in the field give access to real conditions of watering, temperature and light, and allow the possibility to sample percolated water (Nicoara et al., 2014; Bilibio et al., 2017; Constantinescu et al., 2019). In such systems, , some environmental factors cannot be controlled. Mesocosm scale laboratory pilot experiments, as an intermediary step between pot and field experiments, combine the advantage of controlled conditions of temperature, watering and water saturation with the possibility of simultaneously observing the amended and planted surface levels (Valentin-Vargas et al., 2014) and the underlying non saturated and saturated zones (Thouin et al., 2017; 2018).

Among the multiple parameters evaluated during these multi-scale experiments, microbial communities can give indications on the biogeochemical processes. Phytostabilization always induces modifications of the microbial diversity and metabolic profiles in the mining wastes colonized by plants, amended or not (Asemaninejad et al., 2020). The ability of diverse bacterial and fungal species to thrive in mining residues improves soil functions and encourages sustainable plant growth (Harris et al., 2009). Common effects of phytostabilization on microbial diversity were observed in diverse conditions of amendments and plants species, both in greenhouse experiments (Mendez et al., 2007, You et al., 2018) or field conditions (Li et al., 2015; Asemaninejad et al., 2020). They include increases in microbial diversity, biomass and relative increase of heterotrophic/organotrophic genera versus litho-autotrophic organisms.

These last organisms, mainly sulfur and iron oxidizers, are common hosts of mining wastes and contribute to environmental issues linked to production of sulfuric acid and mobilization of metals, thus a decrease of their abundance and activity in mine waste dumps, during phytostabilization, should be beneficial (Valentín-Vargas et al., 2018).

However, most of the previous studies provided data on the microbial communities of the surface environment, in the rhizosphere, and in the close non saturated zones. Thus, the influence of re-vegetation on the underlying microbial communities and on the main biogeochemical cycles driving the fate of pollutants in the depth of the heaps is not well documented.

A methodology to promote stabilization of metals and plant growth with amendments, in the surface of aged tailings from a former lead (Pb)-silver (Ag) mine tailing, was previously developed through microcosm scale experiments (Thouin et al., 2019). The objectives of the present laboratory pilot experiment were to evaluate in environmental compartments rarely studied, from the surface to the water saturated level, the influence of amendments and plants growth on temporal evolution of (1) pore water physico-chemistry, and (2) microbial diversity along the vertical profile of this tailing.

# 2 Material and methods

## 2.1 Characteristics of the mine tailings, the amendments and the plants

Tailings from the site of the former Ag and Pb mine at Pontgibaud (Puy de Dôme, France) were used for the pilot-scale experiment. Mine tailings were sampled to a depth of 0–60 cm from a mine waste heap, using a power shovel (SM1a). Residues were taken in 7 discrete zones within a 25 $m^2$ area. The material was homogenized and sieved at 2 cm; it presented the following particle size distribution: 7% (by weight) < 60 µm, 15% in the 60–315 µm range, and 78% >315

µm. The detailed characteristics of this moderately acidic sandy material are given in Thouin et al. (2019) and Table 1. The pH of the tailings – consisting mainly of quartz, orthoclase and phyllosilicate – was 4.9 (measured in water according to ISO 10390). Tailings contain about 2.6% Pb and Pb bearing phases were detected by X-ray diffraction (XRD): anglesite ($PbSO_4$) and beudantite ($(PbFe_3(AsO_4)(SO_4)(OH)_6$).

*Table 1. Main chemical characteristic of the tailings, ochre, manure and biochar. ([a])* pH was *measured in water according to ISO 10390. ([b]) Element concentrations in solids were analyzed by high resolution inductively coupled plasma mass spectrometry and elemental flash pyrolyser. ([c]) Standard leaching test was performed with demineralized water according to ISO/TS 21268–2. Pb, Ba and As were analyzed by oven atomic absorption spectroscopy, and Fe and Zn by flame atomic absorption spectroscopy. DOC and DON were determined using a TOC elemental analyzer.*

| | Tailings | Ochre | Manure | Biochar |
|---|---|---|---|---|
| pH[a] | 4.9 | 8.1 | 9.9 | 9.5 |
| Solid chemical analyses[b] | | | | |
| Pb ($mg.kg^{-1}$) | 26432 | 10.1 | 2.82 | *n.d.* |
| Fe (%) | 1.5 | 26.1 | *n.d.* | *n.d.* |
| Zn ($mg.kg^{-1}$) | 265 | 14717 | 53.8 | *n.d.* |
| Ba ($mg.kg^{-1}$) | 1063 | 69.8 | 78.9 | *n.d.* |
| As ($mg.kg^{-1}$) | 1134 | 505.7 | 0.75 | *n.d.* |
| C (%) | 0.13 | 1.99 | 35.39 | 81.2 |
| N (%) | <LQ | <LQ | 2.47 | 0.6 |
| S (%) | 1.58 | 0.69 | 0.18 | <LQ |
| Standard leaching testing[c] | | | | |
| Pb ($mg.L^{-1}$) | 19.6 | 0.23 | 0.33 | *n.d.* |
| Fe ($mg.L^{-1}$) | <LQ | 0.4 | <LQ | *n.d.* |
| Zn ($mg.L^{-1}$) | 0.17 | <LQ | 0.33 | *n.d.* |
| Ba ($mg.L^{-1}$) | <LQ | <LQ | 0.27 | *n.d.* |
| As ($\mu g.L^{-1}$) | 2.3 | 2.5 | 7.0 | *n.d.* |
| DOC ($mg.L^{-1}$) | 63.5 | 44.1 | 1134.1 | *n.d.* |
| DON ($mg.L^{-1}$) | 8.1 | 4.4 | 131.1 | *n.d.* |

*DOC: dissolved organic carbon, DON: dissolved organic nitrogen, LQ: limit of quantification (SM2) and n.d.: not determined.*

The first amendment used was an oxy-hydroxide sludge, called ochre, collected in a coal mine water treatment in the south of France, mainly composed of 2-6 µm particles. It contained 26.1 % Fe, and had a pH value in water of 8.1 (measured according to ISO 10390 ; Thouin et al., 2019). A poorly crystalline goethite (FeO(OH)) and aragonite ($CaCO_3$) were identified, and the presence of zincite (ZnO) was suspected (Mertz et al., 2021). The second amendment was cow manure, collected from a farm near Orléans (France). Its pH in water was 9.9 (according to ISO 10390). The manure was dried at 30°C, ground in a mortar and sieved at 2 mm before using. The third amendment was biochar, produced from the slow pyrol**ys**is at 500 °C of hardwood biomass (mixture of oak, beech, and hornbeam), followed by a sieving to obtain a particle size

between 0.5 and 1 mm (Norini et al., 2019). The pH in water was 9.5 measured (according to ISO 10390) and the CEC of biochar (using the 0.05 N cobaltihexamine method) was 0.65 $cmol.kg^{-1}$. Chemical composition of amendments are detailed in Table 1.

*Agrostis capillaris* naturally present on the site was selected for this study. Nandillon et al., 2019 showed that this indigenous *A. capillaris* is a metallicolous ecotype, more tolerant to the stress condition of these mine tailings than a commercial non metallicolous ecotype. The seeds of *A. capillaris* were directly sampled on the Pontgibaud mine site close to the tailings sampling site.

## 2.2 Pilot experiment

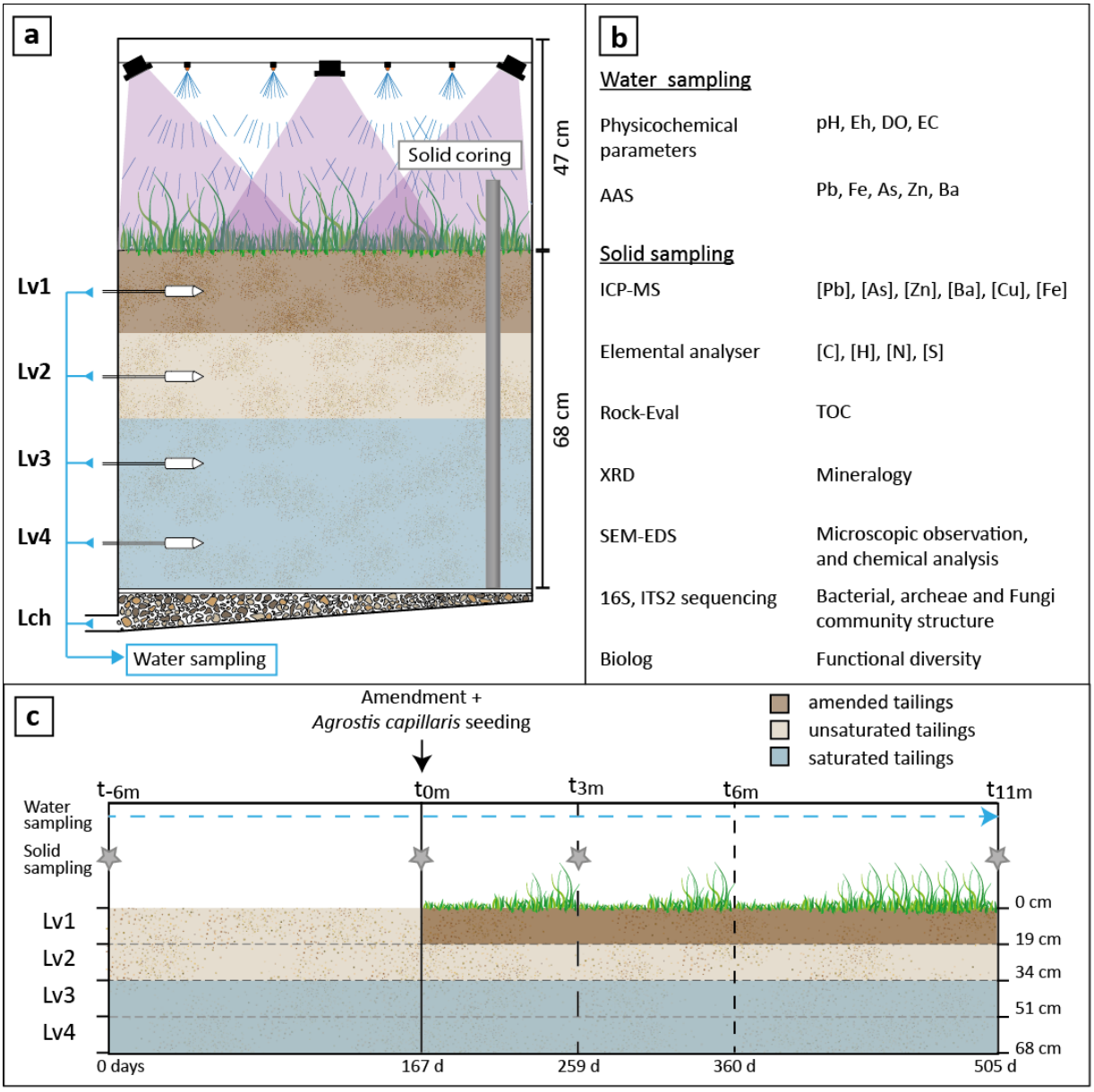


*Figure 1. Design of the laboratory pilot experiment. (a); Analyses performed during the experiment (b) and experimental program presenting the chronology of the main events (c).*

The instrumented laboratory pilot device consisted of a closed stainless-steel column (100 cm in diameter and 145 cm high), placed in a temperature-regulated room at 23 ± 1°C. The pilot design was previously described in Thouin et al. (2017). A layer of inert gravel (centimetric quartz) and a geotextile membrane were placed at the bottom of the column to facilitate outflow drainage without loss of tailing particles. This single metric pilot experiment (Fig. 1), represents

the up-scaling of the assisted phytostabilization method previously developed in multiple microcosms (Thouin et al., 2019).

The column was filled with 814 kg (equivalent to 670 kg of dry weight (dw.)) of the < 2 cm fraction of homogenized mine tailings (SM1b), and was equipped during the process at three levels (Lv2: 26.2 cm, Lv3: 43.7 cm, and Lv4: 61.2 cm measured from the surface and after solids settlement) with time domain reflectrometry probes (TDR) (TRIME-PICO32, IMKO) to measure moisture and temperature in tailings, and with inert Polytetrafluoroethylene/Quartz porous probes (pore size 2 µm, three probes for each depth, regularly spaced) to sample pore water. These probes were inserted into mine tailings at 30 cm from the column wall (Fig. 1a). Five horticultural light-emitting diodes (LED) at the top of the column simulated 12-h day/night cycles. Rainfall was simulated by a sprinkler system connected to a water reservoir and fed by pumps, and consisted in the watering of 5.5 L of Mont Roucous® water each time and three times a week. This mineral water was used because of its chemical composition close to that of rainwater (pH = 6.38, electrical conductivity = 160 µS.cm$^{-1}$, $Cl^-$ = 56 µM, $NO_3^-$ = 24 µM, $SO_4^{2-}$ = 16 µM, $Na^+$ = 109 µM, $K^+$ = 7.7 µM, $Ca^{2+}$ = 25 µM, $Mg^{2+}$ = 21 µM).

After three months of stabilization, the tailings settled by 12.5 % in height, and the thickness of the tailings in the column reached a constant value of 68 cm. The first experimental step corresponded to the control non-phytostabilized condition, which lasted 6 months ($t_{-6m}$ to $t_{0m}$). Both levels Lv4 and Lv3 were always in the saturated part of the column all along the experiment, whereas the Lv2 level was located in the unsaturated zone. The leachate was collected in a steel tank at the bottom, noted Lch, and quantified using scales. This outflow weight as well as moisture and temperature at the three levels (Lv2, Lv3 and Lv4) were continuously monitored.

After 6 months ($t_{0m}$, corresponding to 167 days after starting the monitoring of the experiment, Fig. 1c), 19 cm of tailings surface were stripped (195 kg, equivalent to 173 kg of dw.), and amended with 1 wt% ochre, 1 wt% cow manure and 1 wt% biochar (i.e. 1.73 kg of each amendment), homogenized, then replaced at the top of the column (SM1c). This tailing amended level (Lv1) was instrumented with one TDR and three porous probes at 9.5 cm from the surface, regularly spaced. The amendment was followed by the seeding of 4.1 g of *A. capillaris* on all the tailings surface.

Sampling of pore water from levels Lv1, Lv2, Lv3, Lv4 and Lch was performed (before water sprinkling) via fluorinated ethylene propylene (FEP) tubing connected to a peristaltic pump. The 3 water samples from the 3 independent regularly spaced porous probes of each level (Lv1, Lv2, Lv3 and Lv4) were pooled before determination of physicochemical and geochemical parameters. In Lv1, water sampling was limited due to the low water contents and to the competition with *A. capillaris* roots, this is why there were no water analyses after 231 days.

Solid sampling was performed in the column by coring at $t_{-6m}$, $t_{0m}$, $t_{3m}$ and $t_{11m}$ (at $t_{0m}$ sampling was performed before amendment). Coring was performed with 5 cm diameter and 1m length stainless steel pipes. Only one coring was carried out at each experimental step, in order to minimize disruptive effects. After sampling, the pipes were clogged and put back in place in the tailings to fill the empty space. Each core was separated into four samples, Lv1 at a depth of 0-19 cm, Lv2 at 19-34 cm, Lv3 at 34-51 cm, and Lv4 at 51-68 cm, corresponding to the pore water sampling levels (Fig. 1c). These samples were homogenized, sub-sampled in sterile tubes stored at -20°C for DNA extractions then stored at 5°C in tightly closed sterile jars for the determination of functional diversity of microbial communities.

The sampling of *A. capillaris* biomass and rhizospheric and non-rhizospheric materials were performed at $t_{3m}$, $t_{6m}$ and $t_{11m}$, (respectively 92, 193 and 338 days after seeding). Five plastic (polystyrene) tubes with an area of 19.6 $cm^2$ and a height of 7 cm were used to make small

cores of level Lv1. For each sampled *A. capillaris*, non-rhizospheric (Lv1 NR) tailings fraction was separated from rhizospheric (Lv1 R) materials by shaking, and rhizospheric-associated tailings particles were manually isolated from *A. capillaris* roots. The plants of *A. capillaris* were washed with 0.5 mM $CaCl_2$ and deionized water and plant biomass was measured after plant drying at 60°C during 48h (roots and leaves separately). The total plant cover of the tailings surface was estimated by eye in percentage and was used to extrapolate the total biomass of *A. capillaris* defined in gram of dry leaves and roots by $m^2$. At $t_{3m}$ and $t_{6m}$, the *A. capillaris* plants were cut at about 5 cm above the tailings' surface to simulate mowing and leaves were recovered.

### 2.3 Water analyses

Electrical conductivity (EC), redox potential (Eh), pH, dissolved oxygen (DO), and temperature of interstitial water were measured with a benchtop meter (multiparameter analyser C3040, Consort) connected to an ORP sensor (platinum electrode, with an Ag/AgCl reference electrode, 3M KCl, Eh value refers to the normal hydrogen electrode (NHE)), oxygen probes (Fisherbrand), pH electrode (Fisherbrand) and conductivity probe (Sentek) (Fig. 1b, SM2). As, Pb and Ba were analyzed by oven atomic absorption spectroscopy (AAS) (Varian AA220Z), and Zn and Fe by flame AAS (Varian AA22FS) (SM2).

### 2.4 Analyses of solids

#### 2.4.1 Mineralogy and chemical composition

Solid samples were dried and ground to 70 µm in an agate mortar for X-ray diffraction (XRD) and chemical analyses (SM2). XRD was performed using an INEL CPS120 diffractometer equipped with a Co anode. Measurements of total carbon (C), hydrogen (H), nitrogen (N), and sulfur (S) were obtained using an elemental flash pyrolyser analyzer (Flash 2000, Thermo Fisher Scientific) (SM2). Total organic carbon (TOC) contents were determined by Rock-Eval pyrolysis (Rock-Eval 6 Turbo, Vinci Technologies) (SM2). Elemental concentration

measurements of all solid samples were performed on high resolution inductively coupled plasma mass spectrometry (HR-ICP-MS ; Thermo Element-XR, details in SM2) after complete dissolution by hydrofluoric acid attack ($HNO_3$ 65%, HCl 37% and HF 40%) using a pressurized closed-vessel microwave system (MARS 6, CEM).

### 2.4.2 Optical and SEM-EDS observations

Fresh tailings material sampled in Lv1 at the end of the experiment was observed with a binocular magnifier Leica 2616 APO equipped with a photography and video device and connected to a computer equipped with Leica Mycrosystem software. Scanning electron microscopy coupled with energy dispersive X-ray spectroscopy (SEM-EDS) observations were performed on a TM 3000 (Hitachi) at 15 kV accelerating voltage. SEM was coupled to a SwiftED3000 X-Stream module (Hitachi). The acquisition time of EDS point analyses was 300 seconds and 15 minutes for maps with a resolution of 512 x 384 pixels.

### 2.4.3 DNA extraction and next generation sequencing

Total nucleic acids were extracted in duplicate from 0.5 g (wet weight) of each solid sample with a FastDNA® SPIN Kit for soil (MP Biomedicals, Illkirch, France). DNA was quantified with the Promega Quantifluor®, using the Quantus™ fluorometer (Promega, France).

For next generation sequencing, a fragment of the gene coding 16S rRNA (bacteria and archaea) was amplified using the barcoded, universal primer set (515WF/918WR) (Wang et al., 2009). The primers used to amplify the specific fungal barcode ITS2 were w404 and w40 (Degois et al., 2019). PCR reactions were performed using AccuStart II PCR ToughMix kit and cleaned (HighPrep PCR beads, Mokascience). Pools were submitted for sequencing on Illumina MiSeq instrument at GeT-PlaGe (Auzeville, France). The raw datasets are available on the European Nucleotide Archive system under project accession number PRJEB52405 and PRJEB52412.

Sequences were processed using the FROGS (v.3.0) bioinformatics pipeline (Escudié et al., 2017), implemented into the Genotoul plateform of the Galaxy server of Toulouse. Fastq paired reads were merged with FLASH software, and clustering into OTU with Swarm and an aggregation distance clustering of 3. Chimera and operational taxonomic unit (OTU) with a proportion less than 0.005 % of all sequences were removed. Taxonomic affiliation was performed using BLASTn and the Silva 132 database for 16S rRNA sequences and the Unite Fungi 8.0 database for ITS2 sequences. Filtration on taxonomic affiliation was done at minimum identity of 100% and minimum coverage of 95%. The FROGS pipeline implemented Phyloseq R package was used for OTU structure visualization, rarefaction curves, and alpha diversity index calculations. Chao 1 index (non-parametric measurements) estimates the number of unobserved species from those observed 1 or 2 times while the Shannon and invSimpson diversity indexes give respectively a measure of heterogeneity of microbial community and the probability that two randomly picked individuals do not belong to the same species.

#### 2.4.4 Functional diversity of heterotroph microorganisms

Biolog™ Ecoplates community-level substrate utilization assays were used to study the functional diversity of microbial communities(Garland, 1999). The Biolog™ Ecoplates were incubated at 25 °C and the absorbance values (optical density (OD) at 590 nm) were monitored using an Omega SPECTROstar (BMG Labtech) microplate spectrophotometer at t=0 and 168 h (7 days). The well absorbance values were adjusted by subtracting the average absorbance of the control well (water only) at t=0. After subtracting the control well, an OD590nm > 0.25 was considered as positive. Negative readings (OD < 0) were set to zero for all subsequent analyses.

### 2.5 Statistical analysis

Statistical analysis were performed using R (http://www.r-project.org/ ; version 4.3.0) with the vegan package (version 2.5-7). To visualize differences in the OTUs-based community

composition, we performed an agglomerative hierarchical clustering (AHC) on the 100 most abundant OTUs of 16S rRNA and ITS 2 sequencing data, using Bray-Curtis dissimilarity metric, and Ward's minimum variance. Redundance analysis (RDA) was performed to identify the relationships among samples, environmental variables, and relative abundance of phyla. This analysis was calculated based on Hellinger - transformed phylum abundance basis of 16S rRNA and ITS 2 data (Borcard et al., 2011). Environmental explanatory tested variables were as follows: humidity, pH, TOC, [S], [N], [Fe], [Pb], [Zn], [As], [Cu], [Ba] (solid concentrations at $t_{0m}$, $t_{3m}$, $t_{11m}$) and were standardized. The function ordistep in vegan package was used to identify the significant explanatory forward environmental variable. The significance of the RDA model was tested by ANOVA based on Monte Carlo test with 999 permutations. This analysis helps to determine the most influential factors and the extent that various environmental parameters affected microbial composition.

# 3 Results

## 3.1 Percolated water composition

### 3.1.1 Physico-chemical parameters

Pore-waters in the subsurface levels of the column (Lv2, Lv3, and Lv4) were characterized by constant pH values between 4 and 3, whether before or after the amendment (Fig. 2). In Lch, the pH was higher but decreased from 6 to 4 after amendment of the tailings. In Lv1, the pore water pH was higher than in Lv2, Lv3, and Lv4. Values of redox potential was positive (>300 mV NHE) before amendment, even in the saturated levels (Fig. 2). After amendment, Eh NHE increased in all sampling level and remained positive during the experiment.

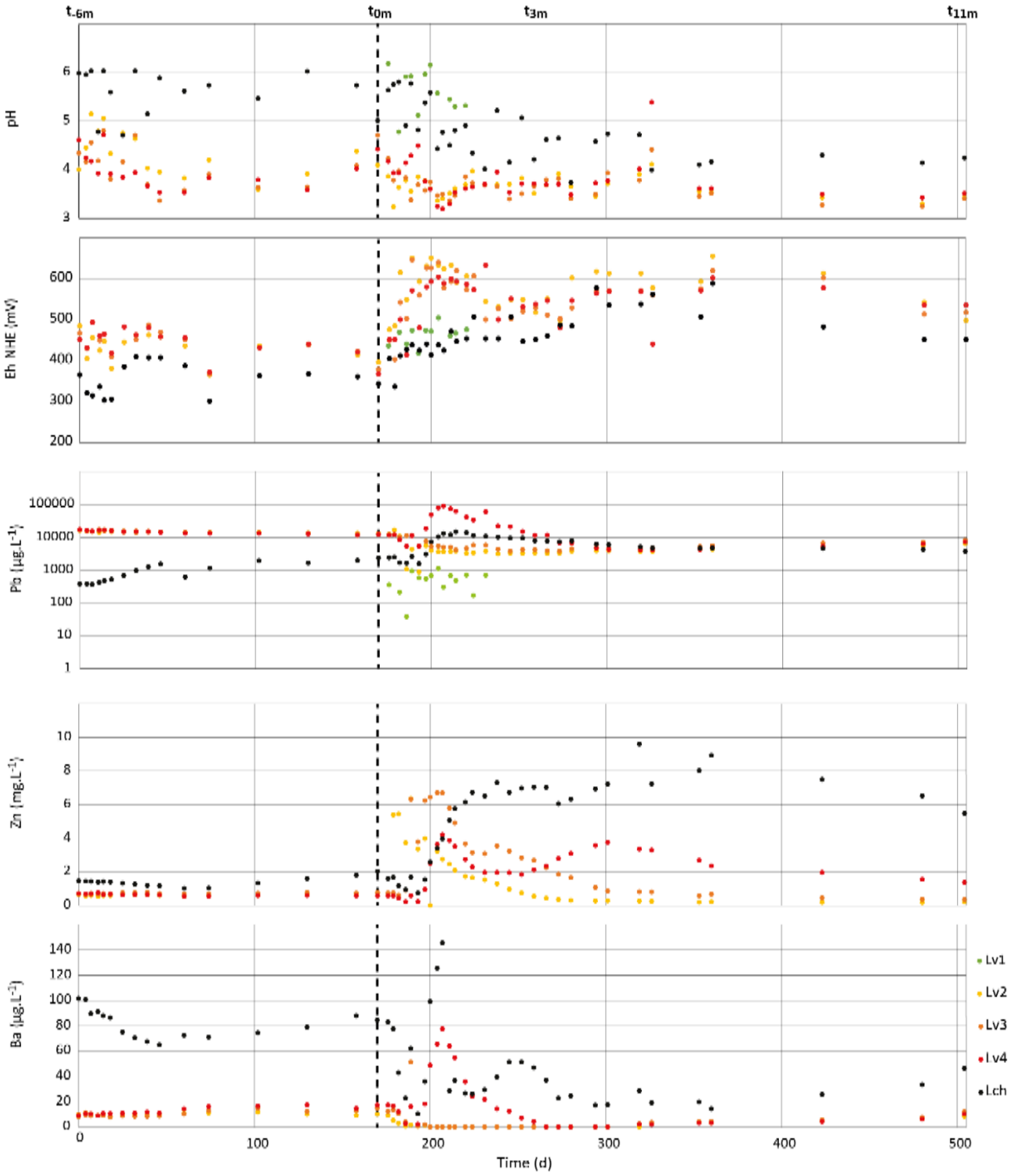


*Figure 2. Evolution of water pH, Eh NHE, Pb, Zn and Ba concentrations in water all along the pilot experiment. Lv1 to Lv4 represent the sampling depths in the tailings. Lv1 was amended and seeded at $t_{0m}$. Lch was the outlet of the pilot.*

### 3.1.2 Metal(loid)s concentrations

Pb was the metal with the highest concentration in tailings' water and leachate. Before $t_{0m}$, Pb concentrations were similar and constant in Lv2, Lv3, and Lv4 with values of 14.4 $mg.L^{-1}$ (Fig. 2). In Lch, Pb concentrations were lower and increased to reach 2.3 $mg.L^{-1}$ just before the amendment. In the amended level Lv1, mean Pb concentration was 532 ± 77 $\mu g.L^{-1}$. In Lv2 and Lv3, Pb rapidly decreased after the amendment to values close to 3 300 and 4 000 $\mu g.L^{-1}$ (respectively), then between $t_{3m}$ and $t_{11m}$, Pb slightly increased to reach 8 160 and 7 150 $\mu g.L^{-1}$ at the end of the experiment. At the bottom of the column, in Lv4, Pb concentration rapidly increased after the amendment to reach a maximum of 88 900 $\mu g.L^{-1}$ on day (d) 207 then decreased down to 4 100 $\mu g.L^{-1}$ on d 319. As for Lv4, Pb concentration in Lch increased after the amendment to reach a maximum of 14 775 $\mu g.L^{-1}$ at d 214 and then decreased down to 3 700 $\mu g.L^{-1}$ at $t_{11m}$.

During the period before the amendment, Ba concentrations were between 8.2 and 18 $\mu g.L^{-1}$ in Lv2, Lv3 and Lv4, and between 101 and 65 $\mu g.L^{-1}$ in Lch (Fig. 2). After $t_{0m}$, Ba concentration rapidly decreased below 2 $\mu g.L^{-1}$ in Lv2 and Lv3, while in Lv4 it increased to a maximum of 77.6 $\mu g.L^{-1}$ on d 207 and decreased under 2 $\mu g.L^{-1}$ on d 300. Between d 300 and the end of the experiment, Ba concentration in Lv2, Lv3 and Lv4 slowly increased to about 10 $\mu g.L^{-1}$. In Lch, two peaks were observed after the amendment, at 207 days (145.6 $\mu g.L^{-1}$) and at 252 (51.4 $\mu g.L^{-1}$).

As concentrations in pore water in Lv2, Lv3 and Lv4 were less than 15 $\mu g.L^{-1}$ throughout the experiment (SM3). In Lch, As concentration decreased from 233 to 13 $\mu g.L^{-1}$ between $t_{-6m}$ and $t_{0m}$. After the amendment As decreased below 5 $\mu g.L^{-1}$ and then increased at the end of experiment to reach 26.7 $\mu g.L^{-1}$.

## 3.2 Evolution of the solids

The evolution of parameters related to organic matter and the main contaminants in solids is presented in Table 2. Amendment slightly increased the concentration in carbon (total C, TOC) in Lv1 and in Lv2, but not at all in the deeper levels Lv3 and Lv4. The other analysed elements did not vary according to experimental time and depth of layer in the column. In particular, Pb, the main contaminant, did not exhibit significant trends as a function of depth and time. One can only note slightly lower Pb contents in the rhizospheric area compared to the non-rhizospheric one. Zn contents slightly increased in the upper levels (Lv1 and Lv2) just after the addition of amendments ($t_{3m}$), due to the presence of Zn in ochre, then returned to values close to that of the tailings.

X-ray diffractograms of the tailings sampled at different depths (Lv1, Lv2, Lv3, and Lv4) at the end of the pilot experiment revealed no change of the mineralogy (SM4): quartz, orthoclase, anglesite, beudantite and a phyllosilicate (presumably muscovite) were the main crystalline phases, as previously identified in the initial tailings (Mertz et al., 2021).

*Table 2 Concentrations of the main interesting constituents in the solids sampled in four depths and at different periods of the pilot experiment, and analyzed by [a] Flash pyrolyzer analyzer, [b] Rock-Eval 6 and [c] HR-ICP-MS.*

| | Depth | C [a] (%) | N [a] (%) | S [a] (%) | TOC [b] (%) | Fe [c] (mg.kg$^{-1}$) | Pb [c] (mg.kg$^{-1}$) | Zn [c] (mg.kg$^{-1}$) | As [c] (mg.kg$^{-1}$) | Cu [c] (mg.kg$^{-1}$) | Ba [c] (mg.kg$^{-1}$) |
|---|---|---|---|---|---|---|---|---|---|---|---|
| $t_{0m}$ | Lv1 | 0.10 | 0.06 | 0.68 | 0.09 | 15 085 | 23 817 | 321 | 1 384 | 124 | 3 631 |
| | Lv2 | 0.09 | 0.06 | n.d. | 0.08 | 19 450 | 24 166 | 327 | 1 398 | 74 | 3 444 |
| | Lv3 | 0.23 | 0.04 | 0.71 | 0.08 | 15 493 | 26 234 | 347 | 1 381 | 131 | 4 635 |
| | Lv4 | 0.04 | 0.02 | 0.72 | n.d. | 15 246 | 22 712 | 381 | 1 319 | 128 | 4 133 |
| $t_{3m}$ | Lv1 R | 1.00 | 0.05 | 1.12 | 0.96 | 14 166 | 19 722 | 521 | 1 127 | 119 | 3 452 |
| | Lv1 NR | 1.04 | 0.04 | 1.05 | 1.02 | 12 793 | 27 594 | 419 | 969 | 107 | 7 706 |

| | | | | | | | | | | | |
|---|---|---|---|---|---|---|---|---|---|---|---|
| | Lv2 | 0.99 | 0.06 | 0.65 | 0.97 | 19 000 | 28 479 | 484 | 1 404 | 69 | 3 974 |
| | Lv3 | 0.18 | 0.06 | n.d. | 0.11 | 17 304 | 27 857 | 371 | 1 598 | 71 | 4 535 |
| | Lv4 | 0.09 | 0.05 | 0.77 | n.d. | 14 336 | 20 848 | 345 | 1 235 | 126 | 4 955 |
| | Lv1 R | 1.28 | 0.07 | 1.04 | 0.98 | 13 280 | 21 644 | 360 | 988 | 101 | 2 503 |
| | Lv1 NR | 1.00 | 0.07 | 0.68 | 0.85 | 16 912 | 29 835 | 308 | 1 083 | 52 | 3 340 |
| $t_{11m}$ | Lv2 | 0.61 | 0.05 | 0.72 | 0.56 | 18 386 | 27 786 | 434 | 1 515 | 73 | 4 321 |
| | Lv3 | 0.15 | 0.03 | 0.70 | 0.11 | 13 935 | 30 940 | 285 | 1 059 | 52 | 3 605 |
| | Lv4 | 0.07 | 0.02 | 0.74 | n.d. | 12 766 | 27 696 | 368 | 1 054 | 91 | 3 051 |

*Initial tailing composition is available in table 1. TOC: total organic carbon, Lv1 to Lv4 represent the sampling depths in the tailings. Lv1 R: solid sampled in the rhizospheric zone, Lv1 NR: solid sampled in the non rhizospheric zone, $t_{0m}$: 6 months after the beginning of the monitoring without amendments and plants, $t_{3m}$: 3 months after adding amendments and seeding Agrostis capillaris, $t_{11m}$: end of the experiment, 11 months after adding amendments and seeding A. capillaris, and n.d.: not determined.*

### 3.3 Agrostis capillaris development

Three months after seeding ($t_{3m}$), thin leaves of *Agrostis capillaris* have grown and a dense implantation with about 80% of surface cover was observed (Table 3). The biomass was about 190 g.m$^2$ for leaves and stems and 57 g.m$^2$ for roots. At $t_{3m}$, *A. capillaris* was cut, and 3 months later, a reduced plant cover (50%) was observed but with larger and better developed leaves. Root biomass has also increased between $t_{3m}$ and $t_{6m}$. A second cut was made at $t_{6m}$. At the end of the pilot experiment, 11 months after seeding, the biomass of aerial parts was multiplied by four (SM1d). *A. capillaris* with stolon was observed and plant cover increased between $t_{6m}$ and $t_{11m}$. Measured root biomass seemed to drastically decrease, but only roots in the first 7 centimeters were weighted whereas roots had colonized the entire thickness of the amended level and were observed up to 40 cm deep.

*Table 3 Agrostis capillaris development. Plant cover was estimated visually and the biomass was measured for a determined surface where the A. capillaris plants were well developed. The extrapolated biomass was determined with biomass and plant cover. * Root biomass was determined only in the first 7 cm.*

| | | **Biomass sampling** | | **Extrapolated biomass** | |
|---|---|---|---|---|---|
| | **Plant cover (%)** | Aerial Parts (g) | Roots* (g) | Aerial Parts (g.m²) | Roots* (g.m²) |
| $t_{3m}$ | 80 | 2.4 | 0.7 | 191.5 | 57.0 |
| $t_{6m}$ | 50 | 2.4 | 1.2 | 119.7 | 73.3 |
| $t_{11m}$ | 70 | 9.8 | 0.2 | 700.9 | 11.4 |

*$t_{3m}$, $t_{6m}$, $t_{11m}$: respectively 3 months, 6 months and 11 months after adding amendments and seeding A. capillaris.*

### 3.4 Tailings stabilization by *Agrostis capillaris* root system

The surface of the tailings at the end of the pilot experiment was visually invaded by the *Agrostis capillaris* root system. The binocular magnifier enabled to observe solid particles forming immobilized tailing aggregates associated with the roots (Fig. 3a). Some fragments of roots observed with SEM-EDS presented fibrous coverage (Fig. 3b) enriched in P and Pb (Fig. 3c point 1) compared with the simple solid particles present at the root surface (Fig. 3c point 2). Fine filaments of 3-4 µm diameter were observed in the rhizosphere (Fig. 3d, e and f). They might be fungal hyphae. EDS mapping revealed the presence of Fe and Pb on their surface and inside their membrane (Fig. 3e point 1, and f).

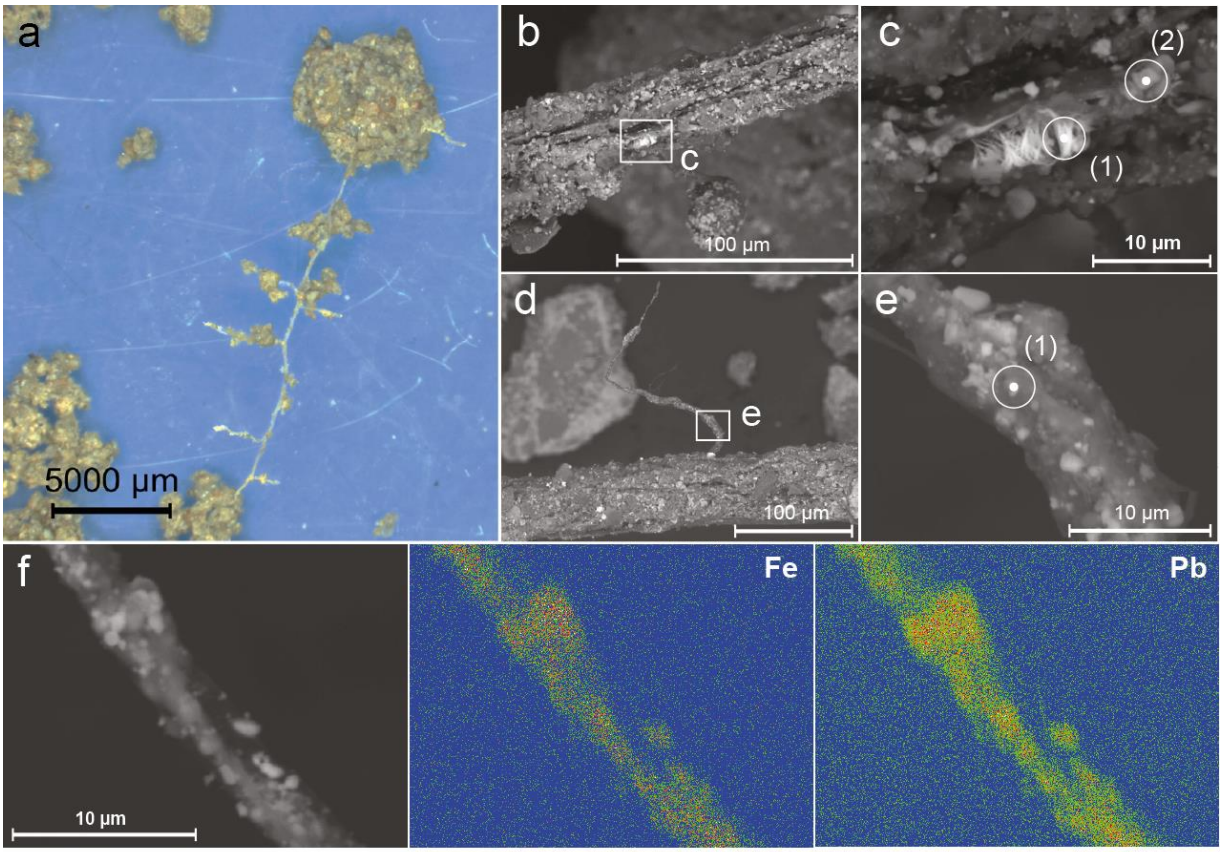


| Relative Concentration (Weight %) | C | O | Mg | Al | Si | P | S | K | Fe | Ba | Zn | As | Pb |
|---|---|---|---|---|---|---|---|---|---|---|---|---|---|
| c)1 | 19.3 | 26.2 | - | 1.2 | 2.7 | 3.5 | 0.7 | 0.6 | 4.2 | 0.2 | 0.2 | 0.4 | 40.0 |
| c)2 | 15.5 | 46.3 | - | 2.2 | 3.8 | 0.5 | 1.2 | 0.5 | 19.0 | - | 0.5 | 2.0 | 8.4 |
| e)1 | 34.5 | 29.3 | 0.2 | 3.9 | 8.5 | 0.3 | 1.9 | 1.7 | 12.5 | - | 0.1 | 0.5 | 6.2 |

*Figure 3. Observations of Agrostis capillaris root samples at the end of the pilot experiment ($t_{11m}$) : (a) aggregates of tailings associated with roots (binocular magnifier); (b) and (c) backscattered electron images of a root (SEM); (d) and (e) backscattered electron images of a presumed fungal hyphae, and (f) backscattered electron images and elemental mapping of Fe and Pb of presumed fungal hyphae; Table present the results of SEM-EDS semi-quantification of elements at the surface of the (c) observed root and (e)inside hyphae membrane.*

## 3.5 Microbial diversity and structure

### 3.5.1 Community species richness and diversity

After treatment steps, a total of 790 820 16S and 920 302 ITS 2 sequences were obtained from the 19 samples. The rarefaction curves reach a plateau for all samples showing that the diversity of communities was well sampled (SM5). The richness of 16S OTUs was homogeneous before amendment at $t_{-6m}$ and $t_{0m}$, with values varying between 431 in Lv3 $t_{-6m}$ and 752 in Lv4 $t_{0m}$. After amendment, an increase of richness was observed except in Lv4 $t_{11m}$. Chao1 index shows

that the majority of OTUs was sequenced (Table 4). The richness of ITS2 sequences was lower than 16S sequences. As with bacteria, the number of OTUs increased after amendment in all levels except in the deepest level at the end of the experiment. The bacterial species diversity, based on the Shannon and InvSimpson indexes (Table 4) increased after amendment in the surface levels Lv1. In Lv2 and Lv3 an increase of diversity indexes was also observed at $t_{3m}$ and $t_{11m}$. The lowest Shannon and InvSimpson indexes were observed in Lv4 at $t_{11m}$. For the fungi, the evolution of Shannon and InvSimpson indexes were less obviously related to the experimental conditions.

*Table 4: 16S and ITS 2 sequences diversities estimation of the solids sampled in four depths and at different periods of the pilot experiment.*

| 16S | | Richness | Chao1 | Shannon | InvSimpson |
|---|---|---|---|---|---|
| $t_{-6m}$ | Lv1 | 576 | 612.7 | 4.2 | 16.4 |
| | Lv2 | 621 | 673.9 | 4.4 | 20.6 |
| | Lv3 | 598 | 635.8 | 4.3 | 18.8 |
| | Lv4 | 752 | 810.1 | 4.4 | 18.6 |
| $t_{0m}$ | Am | 448 | 561.8 | 4.7 | 45.4 |
| | Lv1 | 613 | 652.1 | 4.6 | 28.1 |
| | Lv2 | 549 | 572.8 | 4.1 | 14.8 |
| | Lv3 | 431 | 444.0 | 4.3 | 19.0 |
| | Lv4 | 550 | 595.2 | 4.1 | 15.4 |
| $t_{3m}$ | Lv1 R | 918 | 1022.2 | 5.4 | 86.6 |
| | Lv1 NR | 902 | 997.5 | 5.4 | 85.7 |
| | Lv2 | 953 | 1046.9 | 5.4 | 81.8 |
| | Lv3 | 880 | 986.0 | 4.7 | 28.5 |
| | Lv4 | 938 | 1022.5 | 4.1 | 14.3 |
| $t_{11m}$ | Lv1 R | 747 | 825.5 | 5.2 | 58.4 |
| | Lv1 NR | 829 | 927.3 | 4.9 | 42.1 |

| | | | | | |
|---|---|---|---|---|---|
| | Lv2 | 910 | 1031.9 | 5.4 | 76.2 |
| | Lv3 | 875 | 971.2 | 4.3 | 18.6 |
| | Lv4 | 318 | 366.4 | 3.4 | 14.3 |

| ITS 2 | | Richness | Chao1 | Shannon | InvSimpson |
|---|---|---|---|---|---|
| $t_{-6m}$ | Lv1 | 56 | 61.0 | 2.3 | 4.8 |
| | Lv2 | 51 | 58.5 | 1.9 | 4.2 |
| | Lv3 | 61 | 61.5 | 1.8 | 2.9 |
| | Lv4 | 56 | 63.0 | 2.1 | 4.2 |
| $t_{0m}$ | Am | 91 | 91.1 | 2.3 | 6.4 |
| | Lv1 | 42 | 48.0 | 1.7 | 3.0 |
| | Lv2 | 35 | 45.0 | 2.2 | 5.4 |
| | Lv3 | 26 | 35.3 | 1.8 | 3.4 |
| | Lv4 | 65 | 70.3 | 1.8 | 2.7 |
| $t_{3m}$ | Lv1 R | 107 | 116.2 | 2.2 | 5.2 |
| | Lv1 NR | 105 | 106.9 | 2.6 | 8.4 |
| | Lv2 | 115 | 118.5 | 2.7 | 8.7 |
| | Lv3 | 93 | 93.0 | 2.7 | 7.5 |
| | Lv4 | 82 | 92.0 | 2.8 | 9.7 |
| $t_{11m}$ | Lv1 R | 105 | 115.5 | 2.1 | 3.6 |
| | Lv1 NR | 113 | 117.2 | 3.0 | 13.0 |
| | Lv2 | 117 | 119.5 | 2.5 | 6.2 |
| | Lv3 | 78 | 81.0 | 2.9 | 8.6 |
| | Lv4 | 16 | 22.0 | 2.3 | 8.3 |

*Lv1 to Lv4 represent the sampling depths in the tailings. Am: tailings amended with 1 wt% ochre, 1 wt% cow manure and 1 wt% biochar, Lv1 R: solid sampled in the rhizospheric zone, Lv1 NR: solid sampled in the non rhizospheric zone, $t_{-6m}$: start of the experiment, $t_{0m}$: 6 months after the beginning of the monitoring without amendments and plants, $t_{3m}$: 3 months after adding amendments and seeding Agrostis capillaris, $t_{11m}$: end of the experiment, 11 months after adding amendments and seeding A. capillaris.*

### 3.5.2 Microbial community structure

Samples of solids from the pilot experiment hosted bacterial and fungal communities presenting different spatial and temporal distributions (Fig. 4). The 100 most represented phyla of procaryotes (Fig. 4A) included Proteobacteria, Acidobacteria, Chloroflexi, Bacteroidetes, Gemmatimonadetes, Actinobacteriaceae, Planctomycetes, Cyanobacteria, Firmicutes, members of the Deinococcus-Thermus group for the bacteria, then Thaumarchaeota and Euryarchaeota for the archaea. The AHC analysis, that groups the OTUs according to similarities of occurrence in samples, shows a cluster of OTUs, gathered in the upper part of the Fig. 4A, that were mainly present in the tailings before amendment ($t_{-6m}$ and $t_0$) and in the deepest levels of the column (Lv3 and Lv4) all along the experiment (OTUs n°9 to n°96). The ten most abundant procaryote OTUs (in bold) were present in this group that included Acidobacteria, Chloroflexi, Proteobacteria and Thaumarchaeota, however none of them was identified at the genus level (SM6). Procaryote OTUs more represented in surface levels from $t_{3m}$ to $t_{11m,}$ and influenced by the amendment and plant growth, are grouped in three clusters in the bottom part of Fig. 4A. The cumulative list of the ten most represented known bacterial genera in each sample (SM7), included three sulfur-oxidizing bacteria, namely *Sulfuriferula*, *Sulfurifustis* and *Thiomonas*, and two autotrophic Fe-oxidizing bacteria, i.e. *Gallionella* (only in Lv4 at $t_{3m}$) and *Sideroxydans* (only in Lv4 at $t_{11m}$). All the 44 other major genera are heterotrophic organisms. A known nitrogen fixing genus, *Mesorhizobium*, was present in the list of the 10 most represented procaryote OTUs in Lv1, both in the rhizospheric and non rhizospheric samples. The contribution of the 3 sulfur-oxidizing bacteria, expressed as the sum of their relative abundance in the 10 most abundant identified genera (SM8 and SM9), shows their preponderance in the initial tailings. Their relative abundance strongly decreased in Lv1, Lv2 and Lv3 at $t_{3m}$. At the end of experiment their contribution rose in Lv3 and Lv4.

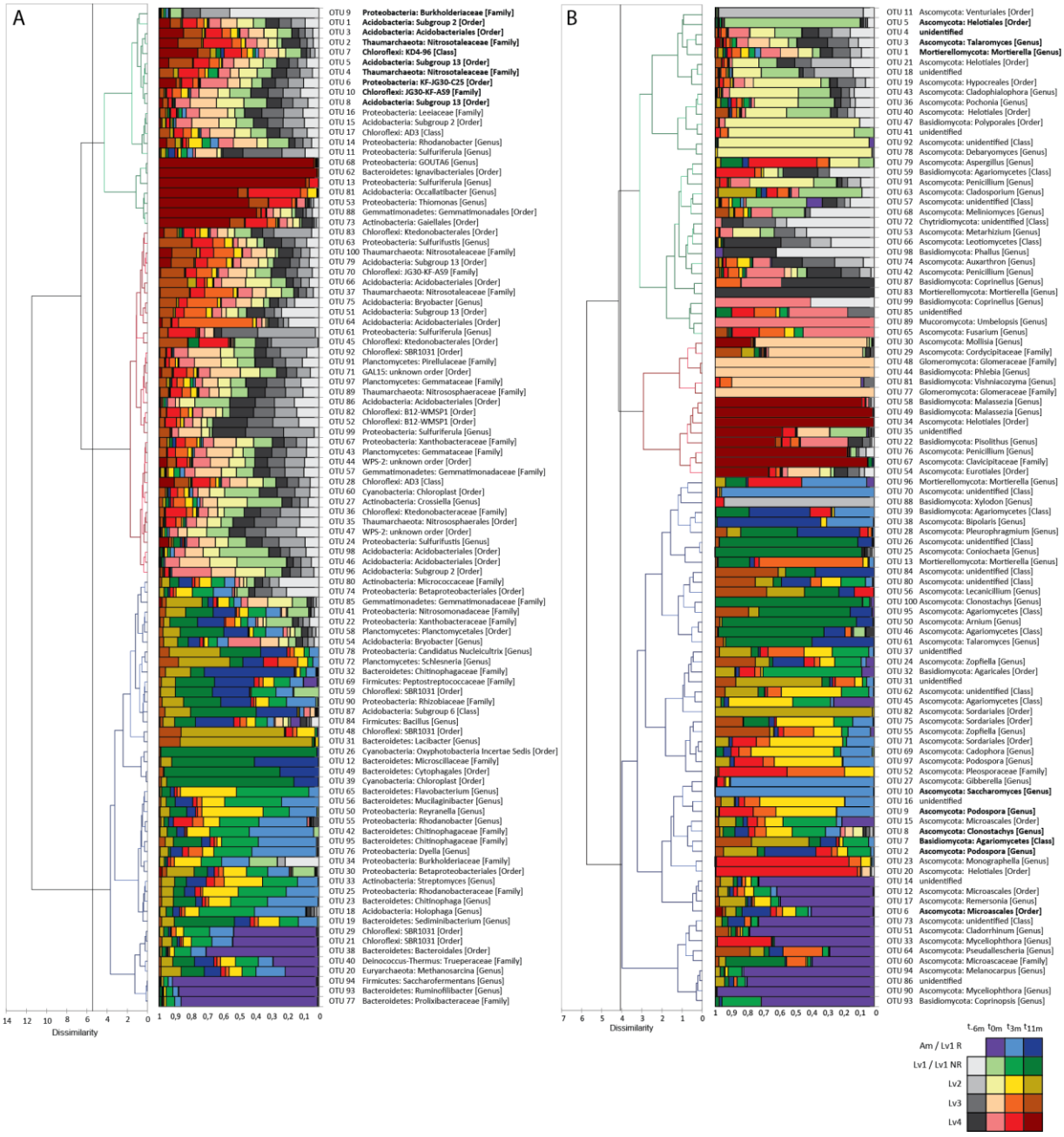


*Figure 4. AHC analysis of the 100 most abundant OTUs (10 most abundant in bold) in solid samples from the pilot experiment. A: bacteria and archaea (based on 16S sequences), B: fungi (based on ITS sequences) (Lv1to Lv4 represent the sampling depths in the tailings, Am: tailings amended with 1 wt% ochre, 1 wt% cow manure and 1 wt% biochar, Lv1 R: solid sampled in the rhizospheric zone, Lv1 NR: solid sampled in the non rhizospheric zone, $t_{-6m}$: start of the experiment, $t_{0m}$: 6 months after the beginning of the monitoring without amendments and plants, $t_{3m}$: 3 months after adding amendments and seeding Agrostis capillaris, $t_{11m}$: end of the experiment, 11 months after adding amendments and seeding A. capillaris).*

The distribution of the 100 most abundant fungal OTUs (Fig. 4B) shows some tendencies already observed with bacterial OTUs, such as a group of fungal OTUs mainly found in the initial tailings, at $t_{-6m}$ in all levels, and $t_{0m}$ from Lv2 to Lv4 gathered at the top of Fig. 4B.

Another group of OTUs was mainly found in the surface levels after amendment ( bottom of Fig. 4B). The 10 most abundant fungal OTUs were distributed between these two groups (Fig. 4B, SM10). A group of fungal OTUs (OTU 14 to OTU 93), probably resulting from the amendment, was found at $t_{3m}$ and $t_{11m}$ in deeper levels (up to Lv3 at $t_{11m}$). The fungi present in the rhizospheric materials at $t_{3m}$ and $t_{11m}$ are different from those found in non rhizospheric Lv1 samples. The classification of the ten most represented known fungal genera (SM11) shows that the genera *Mortierella* and *Talaromyces* were strongly represented in the original tailings ($t_{-6m}$) and detected in all samples. The genera *Clonostachys*, *Coniochae*ta and *Pisolithus* were found among the 12 dominant fungal genera at $t_{-6m}$. The most represented genus in the freshly amended Am Lv1 was *Remersonia*. The genera *Zopfiella* and *Mortierella* were also found in this sample, in small proportions. At $t_{3m}$, the genera *Mortierella*, *Clonostachys* and *Zopfiella* were still present. The genus *Podospora* was present in all levels at this sampling time, , together with *Giberella*, emerging t in Lv1 R and Lv4. The fungal diversity of the rhizospheric Lv1 at $t_{3m}$ differed from that of the other levels, in particular because it was the only level containing *Saccharom*yces as one of the 10 dominant fungal genera. At $t_{11m}$, *Podospora* represented nearly 50% of the fungal genera present in Lv1 R andLv4 exclusively included *Malassezia* as a dominant fungal genera.

A RDA was performed to identify the influence on microbial community structure of 12 physico-chemical characteristics of solid phases (Fig. 5). For Bacteria and Archaea (Fig. 5A) the results indicated that pH, humidity, Zn, and As were explanatory variables that significantly influenced the community structure, which explained 88.6 % ($p = 0.001$) of the total variance. In particular, the highest pH and lowest water content seemed to favour the presence of Bacteroidetes and Proteobacteria, whereas low pH and high water saturation seemed to induce higher proportions of Acidobacteria and Thaumarchaeota. Zn and As concentrations in the solids exerted antagonist influences. For Fungi (Fig. 5B), As and humidity were the only

significant explanatory variables that influenced the community structure. These parameters significantly explain (p = 0.011) 37.7 % of the total variance of fungal community structure. High As concentrations seemed to favorise the development of Mortierellomycota while low water content favorised the presence of Ascomycota.

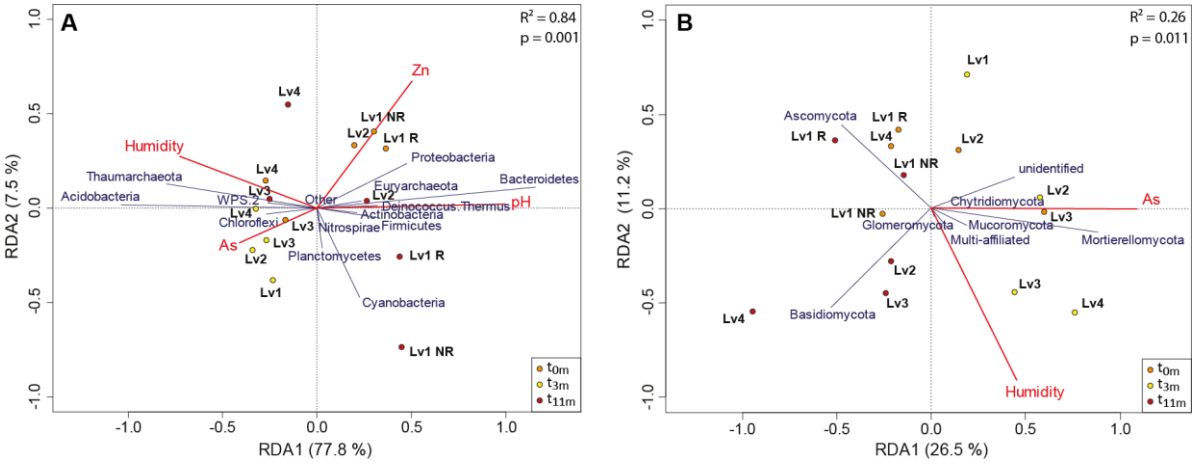


*Figure 5. RDA of sequence abundance assigned at phylum level of microbial communities in the solids samples in relation to environmental variables. A: Bacteria and Archaea (based on 16S sequences), B: Fungi (based on ITS sequences). Red lines represent the significant environmental variable, blue lines represent the Phylum and circles represent the samples. (Lv1 to Lv4 represent the sampling depths in the tailings, Lv1 R: solid sampled in the rhizospheric zone, Lv1 NR: solid sampled in the non rhizospheric zone, $t_{0m}$: 6 months after the beginning of the monitoring without amendments and plants, $t_{3m}$: 3 months after adding amendments and seeding Agrostis capillaris, $t_{11m}$: end of the experiment, 11 months after adding amendments and seeding A. capillaris).*

### 3.5.3 Functional diversity of heterotrophic microorganisms

The substrate spectrum of active cultivable heterotrophs was mainly driven by polymers and carbohydrate degradation in the initial tailings (Fig. 6). Amended surface level clearly displayed higher heterotrophic activities and a deployment of polymer and carboxylic acids degradation was observed at $t_{0m}$. Increase of carboxylic acids biodegradation activities was shared by all levels at $t_{3m}$. A large spectrum of heterotrophic activities was detectable in non-rhizospheric compartments Lv1, Lv2 and Lv3 at $t_{11m}$, when heterotrophic activity was lower in the rhizospheric samples, and nearly inexistent in the deepest level Lv4.

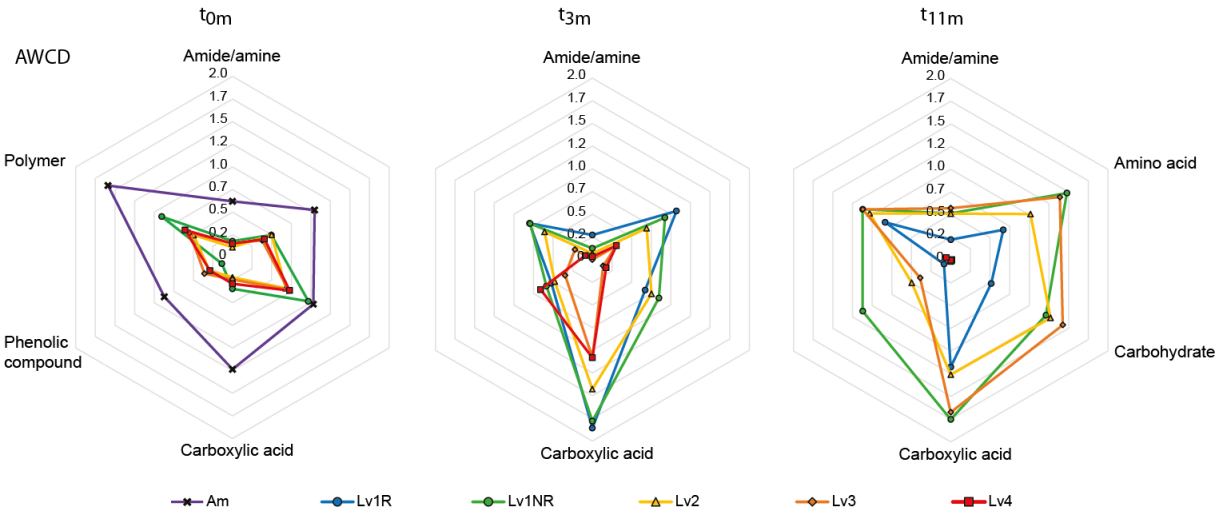


*Figure 6. Functional diversity of cultivable heterotroph microorganisms in solid samples from the pilot experiment (Lv1to Lv4 represent the sampling depths in the tailings, Am: tailings amended with 1 wt% ochre, 1 wt% cow manure and 1 wt% biochar, Lv1 R: solid sampled in the rhizospheric zone, Lv1 NR: solid sampled in the non rhizospheric zone, $t_{0m}$: 6 months after the beginning of the monitoring without amendments and plants, $t_{3m}$: 3 months after adding amendments and seeding Agrostis capillaris, $t_{11m}$: end of the experiment, 11 months after adding amendments and seeding A. capillaris).*

# 4 Discussion

## 4.1 Stabilization of Pb linked to the development of *Agrostis capillaris*

The *Agrostis capillaris* plants grown for 11 months in the column developed an abundant root system that macroscopically retained tailing particles. *A. capillaris* was already reported as a good candidate for phytostabilization, often present as a pioneer plant of polluted sites, resistant to metals and metalloids including Pb and As (Bradshaw, 1952; Meharg and Macnair, 1991; Ernst, 2006; Nandillon et al., 2019). *A. capillaris* has been found to grow spontaneously on contaminated soils, and was recognized as an interesting candidate for the phytostabilization of As and Pb polluted sites (Austry et al., 2013; Rodriguez-Seijo et al., 2016). When using pioneer plants for phytostabilization purposes, preference should be given to pseudo-metallophyte over hyperaccumulator species to minimize the mobilization of metals (Houben et al., 2013). Lead-rich minerals associated with roots of our *A. capillaris* plants were observed by SEM-EDS, co-occurring with high either iron or phosphate concentrations. Pyromorphite ($Pb_5(PO_4)_3(C1)$ or $(OH)^-$ grains have been observed in the outer roots' cell-walls of *A. capillaris* grown in a mine

waste contaminated soil (Cotter-Howells et al., 1999). The authors suggested that the precipitation of Pb phosphate might be related to a mechanism of resistance. As a fact, Nandillon et al. (2019) found higher Pb concentrations in roots of this metallicolous ecotype of *A. capillaris* than in a non-metallicolous one, grown on Pontgibaud tailings, suggesting that Pb immobilization in roots might increase the resistance of plants to this toxic element. Apoplastic sequestration of chloropyromorphite was observed by transmission electron microscopy (TEM) in roots of Pb-resistant *Brachiaria decumbens* (Kopittke et al., 2008).

### 4.2 Impact of phytostabilization on water and solids composition

Amendment of the tailings surface layer was performed to facilitate phytostabilization through the development of *A. capillaris*. This event induced a local increase of solids and pore water pH, accompanied with a decrease of Pb concentration in pore water. This phenomenon, in agreement with results of microcosm experiments (Thouin et al., 2019), was more pronounced in the planted layer, and its amplitude decreased with depth. In the water saturated deeper level Lv4, conversely, a sharp peak of Pb concentration in pore water was observed at the beginning of the phytostabilization process. This phenomenon might be linked to different processes. First, amendment brought several soluble salts releasing cations ($Ca^{2+}$, $Na^{+}$, $Mg^{2+}$ …) that could compete with $Pb^{2+}$ for adsorption on mineral surfaces (Li et al., 2012). This competition might have been compensated by the pH increase in the surface layers, but not in the deeper layer whose pH was not influenced. Another phenomenon that could explain Pb release in Lv4 might be a slight pH decrease linked with the production of $CO_2$ by the organic matter (manure) degradation. This phenomenon was observed at microcosm scale (Thouin et al., 2019) and the associated Pb mobilization was numerically simulated (Mertz et al., 2021). Again, this acidification might have been negligible in the upper levels because of the buffering effect of the amendment, that were not efficient in Lv4.

520 The redox potential in sampled water never decreased significantly, suggesting that reducing
521 processes, such as ferric iron or sulfate bio-reduction, did not establish at a macroscopic scale,
522 whereas they might have occurred locally in micro-environments.

523 Interestingly, Ba behaved in the same way as Pb with a peak of concentration in Lv4 observed
524 following the amendment and seeding. Yet, both Ba and Pb form low-solubility solid phases
525 with sulfate ($PbSO_4$ and $BaSO_4$). In a previous pot experiment (Norini et al., 2019) correlations
526 between Ba and major ions concentrations were highlighted. This could suggest that soluble
527 ions derived from amendment (and more precisely from biochar) induced an increase of Ba
528 concentration in pore water. Zinc release was also observed in all levels except the surface. This
529 might be related both with the transport of Zn-containing ochre in the underlying acidic layers,
530 inducing release of Zn from this amendment, and/or with the release of Zn from the tailings due
531 to competition for adsorption sites with the salts released by amendment (Voegelin et al., 2001).

532 **4.3 Impact of phytostabilization on microbial communities**

533 The development of a plant cover during phytostabilization of mine tailings is generally
534 associated with a diversification of microbial communities in the colonized surface material.
535 This shift can be associated with the amendments provided to help plant growth (Valentin-
536 Vargas et al., 2014), however survey of long-term phytostabilized mine tailings shows that
537 plants alone can induce a complexification of the microbial communities' structure
538 (Asemaninejad et al., 2020). The observed evolutions linked with phytostabilization of mine
539 tailings include the increase of the proportion of heterotrophic bacteria linked to a decrease of
540 the abundance of chemo-autotrophic or mixotrophic bacteria involved in iron and sulfur cycles
541 (Mendez et al., 2007; Valentin-Vargas et al., 2014; Gil-Loaiza et al., 2016; Li et al., 2015), and
542 the development of nitrogen-fixing and plant growth promoting bacteria (Honeker et al., 2019;
543 Asemaninejad et al., 2020). Our moderately acid tailings hosted three main sulfur oxidizers, i.e.
544 *Sulfuriferula*, *Sulfurifustis* and *Thiomonas*, and no FeII-oxidizing acidophiles, whereas many

previous studies reported the occurrence of the genera *Leptospirillum*, *Acidithiobacillus*, *Alicyclobacillus*, *Sulfobacillus*, or *Ferrithrix* (Li et al., 2016; Li et al., 2017; Honeker et al., 2019; Asemaninejad et al., 2020). *Sufuriferula* genus includes the species *Sulfuriferula plumbophilus*, formely *Thiobacillus plumbophilus*, a chemolithotrophic bacterium growing between pH 4.0 and pH 6.5 by oxidation of galena, producing anglesite (Drobner et al., 1992). *Sulfurifustis* genus (Kojima et al., 2015) gathers autotrophic species oxidizing reduced sulfur compounds (thiosulfate, tetrathionate, elemental sulfur) at near neutral pH conditions. *Thiomonas* species are acid-tolerant mixotrophic organisms presenting optimal growth in presence of both organic substrates and sulfur compounds or arsenite (Battaglia-Brunet et al., 2011). The main Pb minerals identified by XRD in Pontgibaud tailings were the oxidized forms anglesite and beudantite. However, a minor fraction of Pb probably remained in the form of the sulfide galena. As a fact, a darker zone that was sampled from the tailing was enriched in Pb, suggesting the presence of less oxidized materials. The absence of acidophilic iron-oxidizing bacteria, that distinguishes our system from many other described autotrophic microbial communities of tailings, may be explained by the low proportion of Fe-bearing sulfides (pyrite and arsenopyrite) compared with galena. Amendment with material providing organic substrates and neutralizing acidity had an immediate effect on microbial communities' composition in the surface level, as previously observed (Valentin-Vargas et al., 2014), with an increase of the proportion of heterotrophic phyla and an activation of the metabolism of organic substrates, in terms of activities and diversity. Moreover, our pilot experiment highlighted the effect of amendments in the underlying zones, with clear changes of global community composition in the non-saturated zone below roots. The two deeper saturated levels were less influenced in terms of global bacterial diversity, however the proportion of sulfur-oxidizers in the 10 most abundant OTUs declined both in Lv2 (non-saturated) and Lv3 (saturated just below) 3 months after the amendment and seeding event. Only the deepest level Lv4 always kept a

570 significant proportion of sulfur-oxidizers. However, at $t_{11m,}$ the proportion of sulfur-oxidizers
571 was restored in Lv3, suggesting an attenuation of the organic substrates supply from the surface.
572 Honeker et al. (2019) already observed re-acidification of phytostabilized mine tailings during
573 phytostabilization, in the initially amended surface levels. Here, we showed a transient
574 influence of surface amendments and plant growth on the underlying levels, however limited
575 spatially as the deeper saturated zone retained the characteristics of initial tailings. From the
576 perspective of Fe cycling, the typical acidophile FeII-oxidizers *Leptospirillum* were not
577 represented in the 100 most abundant OTUs, neither in the 10 most abundant identified genera,
578 however they were detected by the sequencing as minor OTUs typically present in the tailings
579 signature ($t_{-6m}$ and Lv3-Lv4). Two other less acidophile chemolithotrophic FeII-oxidizers,
580 *Gallionella* and *Sideroxydans*, emerged (list of 10 most abundant identified genera) in the
581 deepest level Lv4 at $t_{3m}$ and $t_{11m}$. In parallel, the presence of an acidophilic FeIII-reducer,
582 *Acidibacter*, was noticed (list of 10 most abundant identified genera) in Lv3 at $t_{3m}$ and Lv1R at
583 $t_{11m}$. *Acidibacter* was previously mentioned as part of the acid-generating group in
584 phytostabilized pyritic mine tailings (Honeker et al., 2019). Its presence in our column suggests
585 that amendments and plant growth could induce activation of Fe cycling, including FeIII-
586 reduction in the surface levels fueled by new organic electron donors, providing energy (FeII)
587 for moderately acidophilic FeII-oxidizers in the deepest zones.

588 In the surface level colonized by plants, plant growth promoted bacteria of the genus
589 *Mesorhizobium* which emerged in the 10 most abundant OTUs at $t_{11m}$, suggesting that
590 conditions favorable to long-term plant maintenance were established, and that $N_2$-fixing
591 bacteria could take over from the manure as a source of nitrogen necessary for plant
592 development. Asemaninejad et al. (2020) already observed groups of $N_2$-fixing bacteria
593 including *Mesorhizobium* in long-term vegetated tailings. Bacterial diversity of rhizospheric
594 and non rhizospheric materials did not differ significantly, and evolved similarly from $t_{3m}$ to

595 $t_{11m}$, both in terms of global diversity and representation of the major known bacteria. According
596 to Honeker et al. (2019), the microbial diversity in a phytostabilized soil can be similar in the
597 rhizospheric and bulk soils when pH is near neutral; differences appear when the pH is acidic
598 (<4). In our case, amendment enabled to maintain pH >4 in Lv1 along the experiment. However,
599 differences in the metabolism of organic compounds were observed at $t_{11m}$, the metabolic
600 activity being higher in the bulk than in the rhizospheric material. Whereas root exudates should
601 feed the heterotrophic microbes (Navarro-Noya et al., 2010), here, not the organic substrate
602 availability but other type of limitation of microbial activity might be linked to rhizospheric
603 processes. In particular, phosphate might be depleted in the root vicinity, because of uptake by
604 plants. In a context of low phosphate bioavailability linked to low solubility of Pb phosphate,
605 competition between plants and microbes for this essential nutrient might occur.

606 Concerning fungi, about 90 species of *Mortierella* are known mainly from soil, the rhizosphere,
607 and plant or animal remains in contact with soil (Domsch et al., 1980). Members of *Mortierella*
608 (phylum Zygomycota) are rapidly growing organisms which have been suggested to be
609 saprobes in forest ecosystems (Heitefuss, 2011) and that are important decomposers in soil. The
610 genus *Mortierella* also comprises highly chitinolytic fungi. Due to their potentially endophytic
611 trophic lifestyle, *Mortierella* may be tracking changes in nutrients driven by vegetation turnover
612 (Veach et al., 2017). It is therefore not surprising that this fungal genus was found in the initial
613 tailings that were surrounded by a forest. The adaptive capacities and oligotrophic lifestyle
614 allowed these fungi to be present throughout the experiment. *Talaromyces* are saprotrophic
615 Ascomyceta which contribute to the spoilage of dead or decaying organic material. They are
616 notoriously tolerant to extreme conditions. *Talaromyces* species are commonly distributed in a
617 wide range of substrates, mostly in soil. In an As-contaminated mine soil, Nam et al. (2019)
618 showed that a fungal strain hyper-tolerant to arsenic of *Talaromyces* sp. efficiently removed As
619 from aqueous medium (>70%) with significant improvement by the surface modification of the

fungi with Fe(III) (hydr)oxides. Thus, the hypothesis of a contribution of fungal biomass to the removal of As and/or metals from the pore water of our system cannot be excluded, as our SEM-EDS observations suggested the presence of Fe and Pb at the surface of fungal hyphae. *Pisolithus* is a genus of fungi within the family *Sclerodermataceae*. It is an ectomycorrhizal (ECM) *Gasteromycetes* able to realize symbiosis with various trees (Cairney et al., 2013). We found this genus in Lv1 $t_{0m}$, in the amended level, but also in Lv4 at $t_{0m}$, thus it was not exclusively present in the amendments. This genus was detected in different levels and at different times thereafter. The spores of this ectomycorrhizal fungus were probably initially present in the tailings and were maintained throughout the experiment thanks to their great resistance.

# 5 Conclusion

The first objective of phytostabilization is the decrease of pollutants spreading through surface water runoff and wind erosion. However, the modification of the transfer of metals and metalloids linked with infiltration processes may have important implications in terms of impact on downstream groundwater quality or mine drainage. Here, the phytostabilization technology was examined not only in the surface zones but also from the perspective of the evolution of underlying compartments. The metallicolous *A. capillaris* grew and efficiently trapped tailing particles in its root system. The most mobile pollutant, i.e. lead, was actually stabilized in the surface tailings layer. Beyond these phenomena previously reported for planted tailing systems, our pilot experiment revealed some phenomena occurring in the underlying zones, following the amendment/seeding event, such as a transient increase of the pore water concentrations in Pb, Zn, and Ba. Geochemical data acquired at this laboratory pilot scale will find application in the development of numerical model, helpful to foresee the future evolution of pollutant fluxes in the waste heap. Meanwhile, the phytomanagement process strongly influenced the microbial diversity and metabolic activity in the surface layer but less intensely in the deeper ones. The

main parameters influencing bacterial communities' structure, namely pH and water saturation could be easily related to amendment in the surface compartment, and to the experimental simulation of a groundwater zone. The evolution of fungal community and their potential influence on metalloids and metals dynamics would deserve deeper investigation. Thus, the overall influence of a phytomanagement strategy should be considered and evaluated not only in the surface compartments, but also considering the potential diffusion of phytostabilization-related substances that could influence both abiotic phenomena and microbial processes, toward underlying non-saturated and saturated zones of the mining site.

## CRediT author statement

**Hugues Thouin**: Conceptualization, Methodology, Investigation, Writing-Original draft. **Marie-Paule Norini**: Formal analysis, Investigation, Writing-Original draft. **Fabienne Battaglia-Brunet**: Conceptualization, Supervision, Investigation, Writing-Original draft. **Pascale Gautret**: Conceptualization, Formal analysis, Writing-Review **Marc Crampon**: Formal analysis, Investigation, Writing-Review: **Lydie Le Forestier**: Conceptualization, Supervision, Writing-Review Funding acquisition.

## Acknowledgements

The authors thank Ingrid Girardeau, Louis de Lary de Latour and Stéphane Vaxelaire from the Prevention and Safety in Mines Department (BRGM) and Mikael Beaulieu (BRGM), for their kind help in sampling tailings and iron sludge; Domenico Morabito (LBLGC), Sylvain Bourgerie (LBLGC) and Romain Nandillon (IDDEA) for providing biochar and seeds of *Agrostis capillaris*; Marielle Hatton (ISTO) for CHNS measurements, Rachel Boscardin (ISTO) for Rock-Eval analyses, Nicolas Freslon (ISTO) for HR-ICP-MS analyses, Dominique Breeze (BRGM) for AAS analyses, Mickael Charron (BRGM) for contribution to molecular biology analyses, Jennifer Hellal for English editing and proofreading. This research work was

669 performed within the framework of the Phytoselect project funded by the Région Centre - Val
670 de Loire, contract N°2016-00108485, and by the Labex Voltaire (ANR-10-LABX-100-01). The
671 authors gratefully acknowledge the financial support provided to the PIVOTS project by the
672 Région Centre – Val de Loire: ARD 2020 program, CPER 2015 -2020, and the European Union,
673 which invests in Centre-Val de Loire via the European Regional Development Fund.

674

## References


Acosta, J.A., Abbaspour, A., Martinez, G.R., Martinez-Martinez, S., Zornoza, R., Gabarron, M., Faz, A., 2018. Phytoremediation of mine tailings with *Atriplex halimus* and organic/inorganic amendments: A five-year field case study. Chemosphere 204, 71-78. https://doi.org/10.1016/j.chemosphere.2018.04.027

Asemaninejad, A., Munford, K., Watmough, S., Campbell, D., Glasauer, S., Basiliko, N., Mykytczuk, N., 2020. Structure of microbial communities in amended and unamended acid-generating mine wastes along gradients of soil amelioration and revegetation. Appl. Soil Ecol. 155, 103645. https://doi.org/10.1016/j.apsoil.2020.103645

Al-Lami, M.K., Oustrière, N., Gonzales, E., Burken, J.G., 2018. Amendment-assisted revegetation of mine tailings: improvement of tailings quality and biomass production. Int. J. Phytorem. 21, 425-434. https://doi-org.insu.bib.cnrs.fr/10.1080/15226514.2018.1537249

Austruy, A., Wanat, N., Moussard, C., Vernay, P., Joussein, E., Ledoigt, G., Hitmi, A., 2013. Physiological impacts of soil pollution and arsenic uptake in three plant species: *Agrostis capillaris*, *Solanum nigrum* and *Vicia faba*. Ecotox. Environ. Safety 90, 28-34. https://doi.org/10.1016/j.ecoenv.2012.12.008

Battaglia-Brunet, F., El Achbouni, H., Quemeneur, M., Hallberg, K.B., Kelly, D.P., Joulian, C., 2011. Proposal that the arsenite-oxidizing organisms *Thiomonas cuprina* and '*Thiomonas arsenivorans*' be reclassified as strains of *Thiomonas delicata*, and emended description of *Thiomonas delicata*. Int. J. Syst. Evol. Microbiol. 61, 2816–2821. https://doi.org/10.1099/ijs.0.023408-0

Bilibio, C., Schellert, C., Retz, S., Hense, O., Schmeisky, H., Uteau, D., Peth, S., 2017. Water-balance assessment of different substrates on potash tailings piles using non-weighable

lysimeters. J. Env. Manage. 196, 633-643. http://dx.doi.org/10.1016/j.jenvman.2017.01.024

Borcard, D, Gillet, F, Legendre, P. 2011. Numerical Ecology with R. Springer New York, New York, NY. http://dx.doi.org/10.1007/978-1-4419-7976-6

Bradshaw, A.D., 1952. Populations of *Agrostis tenuis* resistant to lead and zinc poisoning. Nature. 169, 1098. https://doi.org/10.1038/1691098a0

Cairney, John W.G., and Chambers S.M., eds., 2013. Ectomycorrhizal fungi: key genera in profile. Springer Science & Business Media. http://dx.doi.org/10.1007/978-3-662-06827-4

Ciarkowska, K., Hanus-Fajerska, E., Gambus, F., Muszynska, E., Czech, T., 2017. Phytostabilization of Zn-Pb ore flotation tailings with *Dianthus carthusianorum* and *Biscutella laevigata* after amending with mineral fertilizers or sewage sludge. J. Env. Manage. 189, 75-83. http://dx.doi.org/10.1016/j.jenvman.2016.12.028

Constantinescu, P., Neagoe, A., Nicoara, A., Grawunder, A., Ion, S., Onete, M., Iordache, V., 2019. Implications of spatial heterogeneity of tailing material and time scale of vegetation growth processes for the design of phytostabilization. STOTEN 692, 1057-1069. https://doi.org /10.1016/j.scitotenv.2019.07.299

Cotter-Howells, J., Champness, P., Charnock, J., 1999. Mineralogy of Pb-P grains in the roots of *Agrostis capillaris* L. by ATEM and EXAFS. Mineral. Mag. 63, 777-789. https://doi.org/10.1180/002646199548880

Degois, J., Simon, X., Bontemps, C., Leblond, P., Duquenne, P., 2019. Characterization of experimental complex fungal bioaerosols: Impact of analytical method on fungal composition measurements. Aerosol Sci. Technol. 53, 146-159. https://doi.org/10.1080/02786826.2018.1557320

723 Domsch, K.H., Gams, W., Anderson, T.H., 2008. Compendium of Soil Fungi. London:
724 Academic Press. https://doi.org/10.1111/j.1365-2389.2008.01052_1.x

725 Drobner, E., Huber, H., Rachel, R., Stetter, K.O., 1992. *Thiobacillus plumbophilus* spec. Nov.,
726 a novel galena and hydrogen oxidizer. Arch. Microbiol. 157, 213-217.
727 https://doi.org/10.1007/BF00245152

728 Ernst, W.H.O., 2006. Evolution of metal tolerance in higher plants. For. Snow Landsc. Res. 80,
729 3: 251–274. https://www.dora.lib4ri.ch/wsl/islandora/object/wsl:15470

730 Gao, B., Zhang, X.F., Tian, C., Zhang, X.H., Liu, J., 2020. Effects of amendments and aided
731 phytostabilization of an energy crop on the metal availability and leaching in mine tailings
732 using a pot test. Env. Sci. Poll. Res. 27, 2745-2759. https://doi.org/10.1007/s11356-019-
733 07171-x

734 Garland, J.L., 1999. Potential and limitations of BIOLOG for microbial community analysis.
735 In Microbial Biosystems: New Frontiers. Proceedings of the 8th International
736 Symposium on Microbial Ecology (pp. 1-7). Halifax, NS: Atlantic Canada Society for
737 Microbial Ecology.

738 Gil-Loaiza J., White S.A., Root R.A., Solís-Dominguez F.A., Hammond C.M., Chorover J.,
739 Maier R.M., 2016. Phytostabilization of mine tailings using compost-assisted direct
740 planting: Translating greenhouse results to the field. STOTEN 565:451–461.
741 https://doi.org/10.1016/j.scitotenv.2016.04.168

742 Harris, J. A., 2009. Soil microbial communities and restauration ecology: facilitators or
743 followers? Science 325, 573-574. https://doi.org/10.1126/science.1172975

744 Heitefuss R., 2011. Pictorial atlas of soil and seed fungi, morphologies of cultured fungi and
745 key to species. J. Phytopathology, 159, 328. https://doi.org/10.1111/J.1439-
746 0434.2010.01775.X

747 Honeker, L.K., Gullo, C.F., Neilson, J.W., Chorover J., Maier R.M., 2019. Effect of Re-
748 acidification on Buffalo Grass Rhizosphere and Bulk Microbial Communities During
749 Phytostabilization of Metalliferous Mine Tailings. Front. Microbiol. 10, 1209.
750 https://doi.org/10.3389/fmicb.2019.01209

751 Houben, D., Couder, E., Sonnet, P., 2013. Leachability of cadmium, lead, and zinc in a long-
752 term spontaneously revegetated slag heap: implications for phytostabilization. J. Soils
753 Sediments 13, 543-554. https://doi.org/10.1007/s11368-012-0546-5

754 Kojima, H., Shinohara, A., Fukui, M., 2015. *Sulfurifustis variabilis* gen. nov., sp. Nov., a sulfur
755 oxidizer isolated from a lake, and proposal of Acidiferrobacteraceae fam. Nov. and
756 Acidiferrobacterales ord. nov. Int. J. Sys. Evol. Microbiol. 65, 3719-3713.
757 https://doi.org/10.1099/ijsem.0.000479

758 Kopittke, P.M., Asher, C.J., Blamey, F.P.C., Auchterlonie G.J., Guo Y.N., Menzies, N.W.,
759 2008. Localization and Chemical Speciation of Pb in Roots of Signal Grass (*Brachiaria*
760 *decumbens*) and Rhodes Grass (*Chloris gayana*). Environ. Sci. Technol. 42, 4595–4599.
761 https://doi.org/10.1021/es702627c

762 Lago-Vila, M., Arenas-Lago, D., Rodríguez-Seijo, A., Andrade, M.L., Vega, F.A., 2019.
763 Ability of *Cytisus scoparius* for phytoremediation of soils from a Pb/Zn mine:
764 Assessment of metal bioavailability and bioaccumulation. J. Env. Manage. 235, 152-160.
765 https://doi.org/10.1016/j.jenvman.2019.01.058

766 Li, Y., Wang, J., Wang, X., Wang, J., 2012. Adsorption–Desorption of Cd(II) and Pb(II) on Ca-
767 Montmorillonite. Ind. Eng. Chem. Res. 51, 6520–6528.
768 https://doi.org/10.1021/ie203063s

769 Li, X., Bond, P., Van Nostrand, J., Zhou, J., Huang, L., 2015. From lithotroph- to organotroph-
770 dominant: directional shift of microbial community in sulphidic tailings during
771 phytostabilization. Sci. Rep. 5, 12978. https://doi.org/10.1038/srep12978

772 Li, Y., Sun, Q., Zhan, J., Yang, L., Wang, D., 2017. Soil-covered strategy for ecological
773 restoration alters the bacterial community structure and predictive energy metabolic
774 functions in mine tailings profiles. Appl. Microbiol. Biotechnol. 101, 2549–2561.
775 https://doi.org/10.1007/s00253-016-7969-7

776 Li, X., Wang, X., Chen, Y., Yang, X., Cui, Z., 2019. Optimization of combined
777 phytoremediation for heavy metal contaminated mine tailings by a field-scale orthogonal
778 experiment. Ecotoxicol. Environ. Saf. 168, 1-8.
779 https://doi.org/10.1016/j.ecoenv.2018.10.012

780 Meharg, A.A., Macnair, M.R., 1991. The mechanism of arsenate tolerance in *Deschampsia*
781 *cespitosa* (L.) Beauv. and *Agrostis capillaris*. New Phytol. 119, 291–297.
782 https://doi.org/10.1111/j.1469-8137.1991.tb01033.x

783 Mendez, M.O., Glenn, E.P., Maier, R.M., 2007. Phytostabilization potential of quailbush for
784 mine tailings: growth, metal accumulation, and microbial community changes. J.
785 Environ. Qual. 36, 245-253. 10.2134/jeq2006.0197

786 Mendez, M., Maier, R., 2008. Phytoremediation of mine tailings in temperate and arid
787 environments. Rev. Environ. Sci. Biotechnol. 7, 47-59. https://doi.org/10.1007/s11157-
788 007-9125-4

Mertz, S., Le Forestier, L., Bataillard, P., Devau, N., 2021. Leaching of trace metals (Pb) from contaminated tailings amended with iron oxides and manure: New insight from a modelling approach. Chem. Geol. 579, 120356. https://doi.org/10.1016/j.chemgeo.2021.120356

Nam, I.H., Murugesan, K., Ryu, J., & Kim, J.H., 2019. Arsenic (As) removal using Talaromyces sp. KM-31 isolated from as-contaminated mine soil. Minerals 9, 568. https://doi.org/10.3390/min9100568

Nandillon, R., Lebrun, M., Miard, F., Gaillard, M., Sabatier, S., Morabito, D., Bourgerie, S., 2019. Contrasted tolerance of *Agrostis capillaris* metallicolous and non-metallicolous ecotypes in the context of a mining technosol amended by biochar, compost and iron sulfate. Environ. Geochem. Health. 43,1457-1475. https://doi.org/10.1007/s10653-019-00447-8

Navarro-Noya, Y.E., Jan-Roblero, J., del Carmen González-Chávez, M., 2010. Bacterial communities associated with the rhizosphere of pioneer plants (Bahia xylopoda and Viguiera linearis) growing on heavy metals-contaminated soils. Anton. van Leeuwenhoek 97, 335–349. https://doi.org/10.1007/s10482-010-9413-9

Nicoara, A., Neagoe, A., Stancu, P., De Giudici, G., Langella, F., Sprocati, A.R., Iordache, V., Kothe, E., 2014. Coupled pot and lysimeter experiments assessing plant performance in microbially assisted phytoremediation. Environ. Sci. Pollut. Res. 21, 6905-6920. https://doi.org/10.1007/s11356-013-2489-9

Norini, M. P., Thouin, H., Miard, F., Battaglia-Brunet, F., Gautret, P., Guégan, R., Le Forestier, L., Morabito, D., Bourgerie, S., Motelica-Heino, M., 2019. Mobility of Pb, Zn, Ba, As and Cd toward soil pore water and plants (willow and ryegrass) from a mine soil amended

812 with biochar. J. Env. Manage. 232, 117-130.
813 https://doi.org/10.1016/j.jenvman.2018.11.021

814 Ouangrawa, M., Aubertin, M., Molson, J.W., Bussière, B., Zagury, G.J., 2010. Preventing acid
815 mine drainage with an elevated water table: long-term column experiments and parameter
816 analysis. Wat. Air Soil Pollut. 213, 437-458. https://doi.org/10.1007/s11270-010-0397-x

817 Rodríguez-Seijo, A., Lago-Vila, M., Andrade, M.L., Vega, F.A., 2016. Pb pollution in soils
818 from a trap shooting range and the phytoremediation ability of *Agrostis capillaris* L.
819 Environ. Sci. Pollut. Res. 23, 1312–1323. https://10.1007/s11356-015-5340-7

820 Rodriguez, L., Gomez, R., Sanchez, V., Villasenor, J., Alonso-Azcarate, J., 2018. Performance
821 of waste-based amendments to reduce metal release from mine tailings: One-year
822 leaching behaviour. J. Env. Manage. 209, 1-8.
823 https://doi.org/10.1016/j.jenvman.2017.12.031

824 Sikdar, A., Wang, J., Hasanuzzaman, M., Liu, X., Feng, S., Roy, R., Sial, T.A., Lahori, A.H.,
825 Arockiam, J., Parimala, G. S., Wang, X., 2020. Phytostabilization of Pb-Zn Mine Tailings
826 with *Amorpha fruticosa* Aided by Organic Amendments and Triple Superphosphate.
827 Molecules, 25, 1617. https://doi.org/10.3390/molecules25071617

828 Thouin, H., Battaglia-Brunet, F., Gautret, P., Le Forestier, L., Breeze, D., Seby, F., Norini,
829 M.P., Dupraz, S., 2017. Effect of saturation/desaturation cycles and input of natural
830 organic matter on C, N, As and metals biogeocycles in a chemical warfare agents burning
831 impacted soil: a mesocosm study. STOTEN 595, 279-293.https://doi.org
832 /10.1016/j.scitotenv.2017.03.218

833 Thouin, H., Battaglia-Brunet, F., Norini, M. P., Le Forestier, L., Charron, M., Dupraz, S.,
834 Gautret, P., 2018. Influence of environmental changes on the biogeochemistry of arsenic

in a soil polluted by the destruction of chemical weapons: a mesocosm study. STOTEN 627, 216-226. https://doi.org/10.1016/j.scitotenv.2018.01.158

Thouin, H., Norini, M. P., Le Forestier, L., Gautret, P., Moteica-Heino, M., Breeze, D., Gassaud, C., Battaglia-Brunet, F., 2019. Microcosm-scale biogeochemical stabilization of Pb, As, Ba and Zn in mine tailings amended with manure and ochre. Appl. Geochem. 111, 104438.

Valentín-Vargas, A., Root, R.A., Neilson, J.W., Chorover, J., Maier, R.M., 2014. Environmental factors influencing the structural dynamics of soil microbial communities during assisted phytostabilization of acid-generating mine tailings: A mesocosm experiment. STOTEN 500-501, 314-324. https://doi.org/10.1016/j.scitotenv.2014.08.107

Valentín-Vargas, A., Neilson, J. W., Root, R. A., Chorover, J., Maier, R. M., 2018. Treatment impacts on temporal microbial community dynamics during phytostabilization of acid-generating mine tailings in semiarid regions. STOTEN 618, 357-368. https://doi.org/10.1016/j.scitotenv.2017.11.010

Veach, A.M., Stokes, C.E., Knoepp, J., Jumpponen, A., Baird, R., 2017. Fungal communities and functional guilds shift along an elevational gradient in the southern appalachian mountains. Microb. Ecol. 76, 156-168. https://doi.org/10.1007/s00248-017-1116-6

Voegelin, A., Vulava, V. M., Kretzschmar, R., 2001. Reaction-Based Model Describing Competitive Sorption and Transport of Cd, Zn, and Ni in an Acidic Soil. Environ. Sci. Technol. 35, 1651–1657. https://doi.org/10.1021/es0001106

Wang Z, Tollervey J, Briese M, et al (2009) CLIP: Construction of cDNA libraries for high-throughput sequencing from RNAs cross-linked to proteins in vivo. Methods 48:287–293. https://doi.org/10.1016/j.ymeth.2009.02.021

Yang, S., Cao, J., Li, F., Peng, X., Peng, Q., Yang, Z., Chai, L., 2016. Field evaluation of the effectiveness of three industrial by-products as organic amendments for phytostabilization of a Pb/Zn mine tailings. Environ. Sci.: Processes Impacts 18, 95-103. https://doi.org/10.1039/c5em00471c

Ye, Z.H., Shu, W.S., Zhang, Z.Q., Lan, C.Y., Wong, M.H., 2002. Evaluation of major constraints to revegetation of lead/zinc mine tailings using bioassay techniques. Chemosphere 47, 1103-1111. https://doi.org/10.1016/s0045-6535(02)00054-1

You, F., Dalal, R., Huang, L., 2018. Biochar and biomass organic amendments shaped different dominance of lithoautotrophs and organoheterotrophs in microbial communities colonizing neutral copper(Cu)-molybdenum(Mo)-gold(Au) tailings. Geoderma 309, 100-110. https://doi.org/10.1016/j.geoderma.2017.09.010